Accepted Manuscript

Synthesis and evaluation of third generation vitamin D3 analogues as inhibitors of Hedgehog signaling

Chad A. Maschinot, Lianne Q. Chau, Robert J. Wechsler-Reya, M. Kyle Hadden

PII: S0223-5234(18)30987-5

DOI: https://doi.org/10.1016/j.ejmech.2018.11.028

Reference: EJMECH 10885

To appear in: *European Journal of Medicinal Chemistry*

Received Date: 13 September 2018

Revised Date: 9 November 2018

Accepted Date: 9 November 2018

Please cite this article as: C.A. Maschinot, L.Q. Chau, R.J. Wechsler-Reya, M.K. Hadden, Synthesis and evaluation of third generation vitamin D3 analogues as inhibitors of Hedgehog signaling, *European Journal of Medicinal Chemistry* (2018), doi: https://doi.org/10.1016/j.ejmech.2018.11.028.

Synthesis and Evaluation of Third Generation Vitamin D3 Analogues as Inhibitors of Hedgehog Signaling

Chad A. Maschinot[1†], Lianne Q. Chau[2], Robert J. Wechsler-Reya[2], M. Kyle Hadden[1,]*

[1] Department of Pharmaceutical Sciences, University of Connecticut, 69 North Eagleville Road, Unit 3092, Storrs, CT 06269, United States

[2] Tumor Initiation and Maintenance Program, NCI-Designated Cancer Center, Sanford Burnham Prebys Medical Discovery Institute, 10901 North Torrey Pines Road, La Jolla, CA 92037, United States

KEYWORDS: Hedgehog; Vitamin D; Basal Cell Carcinoma; Medulloblastoma; Gli.

ABSTRACT

The Hedgehog (Hh) pathway is a developmental pathway with therapeutic potential as a target for a variety of cancers. In recent years, several vitamin D-based compounds have been identified as potent inhibitors of Hh signaling. These analogues contain aromatic phenol A-ring mimics coupled to the CD-ring side chain of vitamin D3 through modified *seco*-B regions. To continue structure-activity relationship studies on this class of Hh pathway inhibitors, multiple series of vitamin D-based analogues that contain an amine-based *seco*-B tether and/or incorporate a hydroxyl moiety on C-25 were designed and synthesized. These compounds were evaluated in multiple cell lines for their anti-Hh activity, and we identify analogues **16**, **21**, **22** as potent vitamin D-based Hh inhibitors (IC_{50} values of 110 - 340 nM). We also performed a series of mechanism of action studies in knockout cell lines to further explore whether these analogues inhibit the Hh pathway through a known Hh pathway component or the vitamin D receptor. While the specific cellular target that mediates these effects remains elusive, our studies suggest multiple cellular targets may mediate the anti-Hh activity of this scaffold.

1. Introduction

Aberrant signaling of the Hedgehog (Hh) pathway has been associated with a variety of disease states from osteoporosis to several forms of cancer, including basal cell carcinoma (BCC) and medulloblastoma (MB) [1-3]. The pathway is composed of two transmembrane receptor proteins, Patched (Ptch) and Smoothend (Smo), as well as multiple cytosolic proteins, including Suppressor of Fused (SuFu) and the glioma associated oncogene (Gli) family of transcription factors. Multiple small molecule inhibitors of Hh signaling are under preclinical and clinical development, and two Smo antagonists, Vismodegib and Sonidegib, have been approved by the FDA for metastatic BCC [3]. The development of acquired resistance and relapse to Vismodegib and Sonidegib [4-5] has prompted the continued search for alternative Hh pathway inhibitory scaffolds. Multiple approaches are currently being investigated that target both canonical (Smo and Gli) and non-canonical signaling [6].

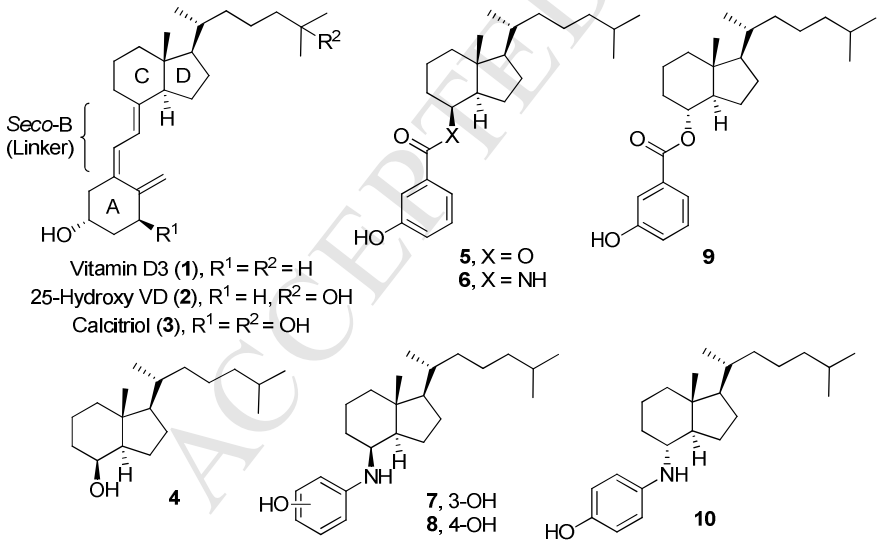

Fig 1. Vitamin D-based inhibitors of Hedgehog signaling.

Among the scaffolds under investigation for their anti-Hh activity is the vitamin D-based family of pathway inhibitors (Fig. 1). As naturally occurring metabolites, the canonical vitamin

D signaling pathway is well studied and is traditionally associated with calcium homeostasis via the 'active' hormone calcitriol (**3**), which functions through binding to and activation of the vitamin D receptor (VDR) [7].

Following the initial reports of Hh inhibition by vitamin D3 (VD3, **1**) [8-10], we have characterized several VD3-based small molecules that selectively inhibit Hh signaling [11-14]. Initial structure-activity relationship (SAR) studies for this scaffold focused on **1** as our lead compound because it showed minimal VDR agonism compared to **2** and **3**. The first series of analogues incorporated an aromatic A-ring moiety coupled to the natural CD-ring of **1** (**4**) through an ester linker (**5**), which greatly increased selectivity and potency compared to **1** [11]. When the *seco*-B region was investigated further, an increase in potency was observed with the use of nitrogen containing (amine) tethers (**6** – **8**) [13]. Additionally, inversion of the C-8 stereocenter from the α- to β-orientation did not show a significant effect on inhibitory activity [13]. Herein, we report further SAR for this scaffold with a particular focus on expanding our amine-linked analogues while also incorporating the C-25 hydroxyl moiety present in calcitriol. In addition, we have utilized several knockout cell lines to provide initial evidence of cross-talk between VDR and the Hh pathway.

2. Results and discussion

2.1. Analogue design rationale

One of the most notable observations from our previous SAR was that reducing the *seco*-B linker region from two atoms (**5** and **6**) to a single atom (**7** and **8**) altered the most potent A-ring hydroxyl position from *meta* (**7**) to *para* **(8)**. A second notable observation was that little difference in activity was demonstrated between the α- (**8**) or β-orientations (**10**) of the linker

region suggesting there may be no preference for a specific orientation of the C-8 stereoisomer. With these differences in mind, we envisioned a new series of analogues to further evaluate (1) whether other observations from our ester analogues [11] were applicable to compounds containing an amine in the *seco*-B region (**12** – **16**) and (2) whether extension of the nitrogen-containing linker back to two atoms by the addition of a methylene group would affect the inhibitory activity (**18** – **19**).

Our initial evaluation of these nitrogen-based linker analogues indicated that the free A-ring hydroxyl group was required and provided the foundation for a second series of analogues in which a C-25 hydroxyl group was introduced (**21** – **22**, **27** – **28**). Previous reports from our research and others [9-14] demonstrated that both **2** and **3** are more potent inhibitors of Hh signaling compared to **1**; therefore, we synthesized a series of analogues that could both increase potency of the scaffold while also providing potential probes to evaluate crosstalk between VDR and Hh signaling [15]. Finally, a series of analogues that masked the C-25 hydroxyl as the methyl ether (**25**, **31**, **34**) were synthesized and evaluated to determine whether the increased anti-Hh activity associated with our initial C-25 hydroxylated compounds could be maintained while reducing the VDR activation that results from addition of the hydroxyl group.

2.2. Analogue synthesis

Synthesis of the amine linker analogues is centered on the one pot reductive amination of the desired amine with Grundmann's ketone (**11**) or the extended aldehyde **17**. Following previously described protocols [11], **11** is obtained in two steps from VD3 via global ozonolysis and oxidation of **4** (Scheme 1). Reductive amination of **11** with sodium triacetoxyborohydride in the presence of the requisite amine yielded corresponding amines **12** – **16**. To extend the linker,

aldehyde **17** was obtained in high yield following hydrolysis of the enol ether obtained through a Wittig reaction between **11** and methoxymethyl triphenylphosonium chloride. The same reductive amination procedure was applied to **17** to provide extended amines **18** – **19** (Scheme 1).

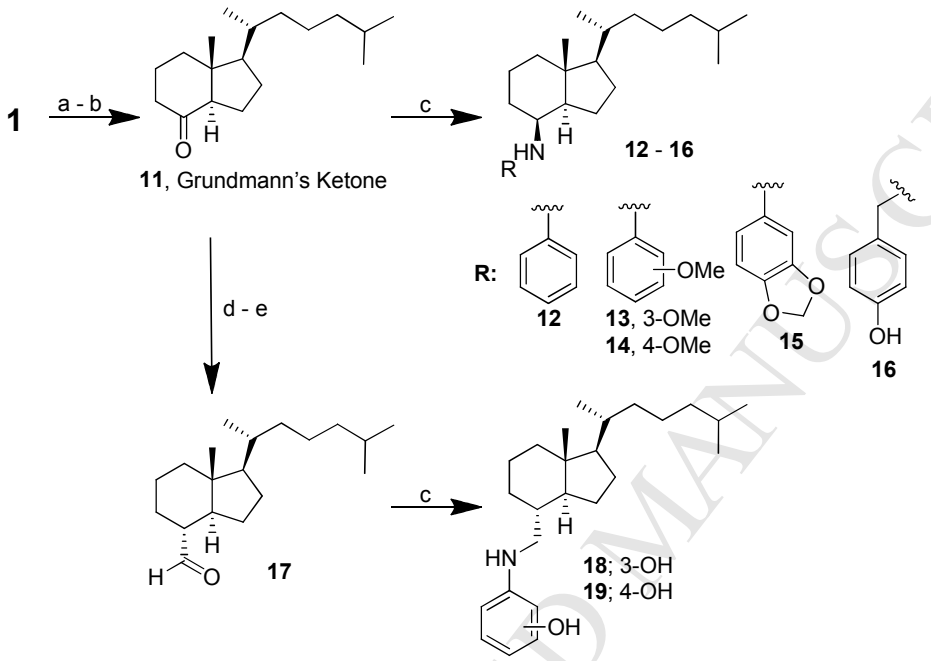

Scheme 1. Synthesis of amine *seco*-B analogues of vitamin D3. Reagents and Conditions: (a) i. O_3, pyridine, DCM:MeOH (3:1), 0 °C to RT; ii. $NaBH_4$; 92% over two-steps (b) PDC, DCM; 96 % (c) $NaBH(OAc)_3$, AcOH, R-amine, DCE; 20 – 65% (d) $PPh_3Cl(MeOMe)$, NatBuO, THF, 0 °C to RT; 89% (e) 2N HCl, MeOH, 60 °C; 75%.

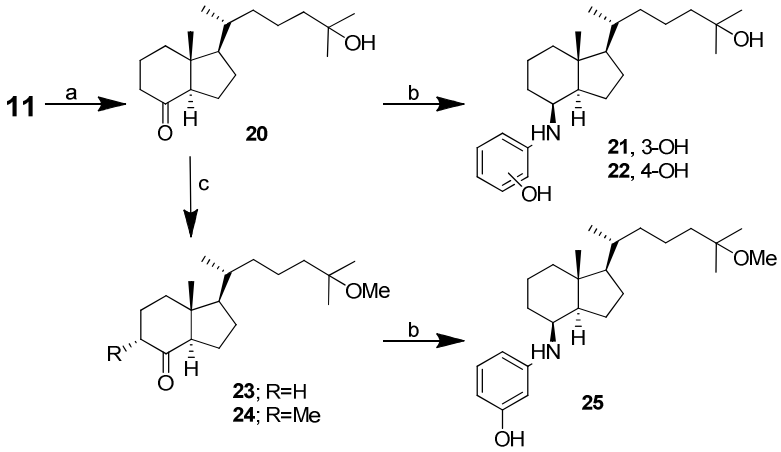

Scheme 2. Synthesis of C-25 functionalized single atom nitrogen containing *seco*-B analogues. Reagents and conditions: (a) $RuCl_3$, $NaIO_4$, pyridine, MeCN:H_2O, 60 °C; 67% (b) $NaBH(OAc)_3$, AcOH, R-amine, DCE; 15 – 35 % (c) MeI, NaH, DMF, 0 °C; 17 – 25 %.

Introduction of the C-25 hydroxyl was performed using ruthenium (III) chloride and sodium periodate for the *in-situ* generation of ruthenium tetroxide (Scheme 2) [16]. Due to steric hindrance of **11**, specifically interactions between C-18 and C-20, selective hydroxylation at the C-25 position provided **20** in good yield (65%). Hydroxylated amines **21** and **22** were obtained from **20** through the reductive amination procedure described above. Conversion of the C-25 hydroxyl to the methyl ether (**23**) was performed using methyl iodide and sodium hydride. Our desired product was obtained in low yield due to concomitant α-methylation at C-9 (**24**). Most likely, α-methylation at C-9 occurs following the desired etherification due to the presence of **23** and the 'dimethylated' byproduct **24** (the 25-OH, C-9 α-methyl compound was not observed). Reductive amination of **23** provided **25** in modest yield.

Reductive amination of aldehyde **26** yielded **27** and **28**, C-25 hydroxylated analogues of **18** and **19**, respectively (Scheme 3). Since the C-9 methylated byproduct (**23**) was the major product observed during the etherification of **20**, addition of the methyl ether group to the aldehyde was performed following its conversion to the methoxy enol ether to afford **29** (Scheme 3). The yield of **29** was significantly increased through this route compared to our initial preparation of **23**.

Following hydrolysis of **29** to its corresponding aldehyde (**30**), reductive amination with 3-aminophenol yielded amine **31**.

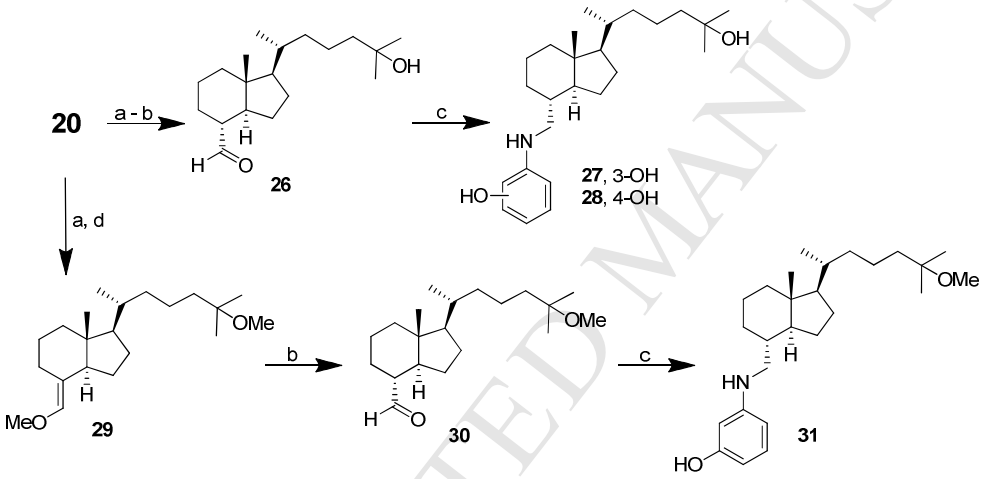

Scheme 3. C-25 functionalization of two atom amine-linked analogues. Reagents and conditions: (a) $PPh_3Cl(MeOMe)$, NatBuO, THF; 89 % (b) 2N HCl, MeOH, 60 °C; 60 - 75% (c) $NaBH(OAc)_3$, AcOH, R-amine, DCE; 32 – 59 % (d) MeI, NaH, DMF, 0 °C; 62%.

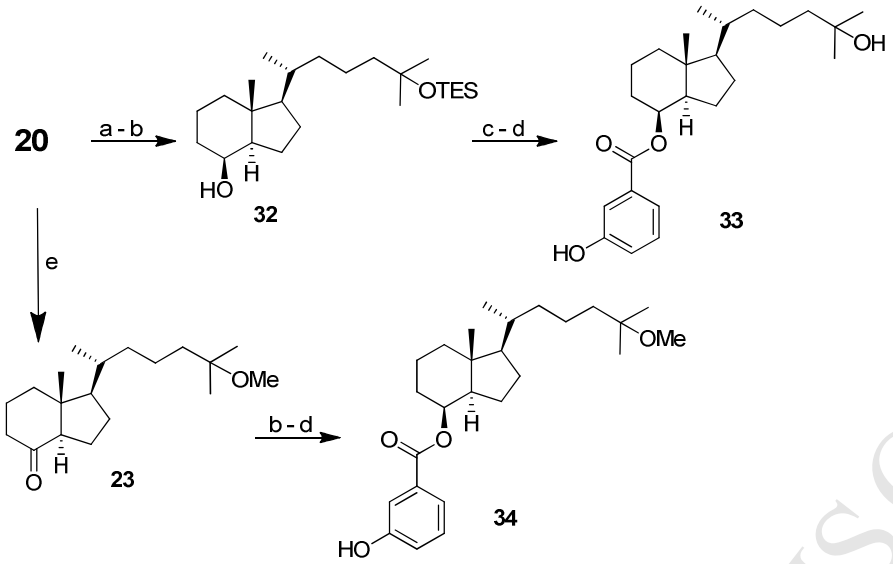

Scheme 4. C-25 functionalized ester analogues. Reagents and conditions: (a)TES-Cl, imidazole, DMF; 94% (b) $NaBH_4$, MeOH:DCM; 88 - 92% (c) 3-OMOM-benzoic acid, DCC, DMAP, DCM; 52 - 70% (d) CSA, MeOH; 60 - 75% (e) MeI, NaH, DMF, 0 °C; 35%.

Ketone **20** provided the starting material for the synthesis of C-25 hydroxylated ester **33**. Protection of the C-25 hydroxyl group as the triethyl silyl ether (TES) followed by sodium borohydride reduction gave alcohol **32** (Scheme 4). Triethyl silane provided a useful protecting group because following esterification with the MOM-protected 3-hydroxybenzoic acid, both protecting groups could be removed simultaneously with camphor sulfonic acid (CSA) to afford analogue **33**. In a similar fashion, ester **34** was obtained in three steps from ketone **23**.

2.3. Biological evaluation

2.3.1. SAR and Preliminary Pharmacokinetic Analysis.

The initial evaluation of VD3 analogues as Hh pathway inhibitors was performed in C3H10T1/2 cells, an Hh-dependent mouse embryonic fibroblast (MEF) cell line. In addition, we previously reported significant upregulation of the VDR target gene Cyp24A1 following VDR activation in these MEF cells, allowing for dual observations of potency and selectivity in this cellular model

[11-14]. Following our previously utilized procedures, the Hh target gene Gli1 was upregulated in the MEFs via endogenous administration of oxysterols (OHCs; 20(*S*)-OHC and 22(*S*)-OHC at 5 μM each), which are well-characterized agonists of Hh signaling. Inhibition of Hh signaling (Gli1 downregulation) and activation of VDR (upregulation of Cyp24A1) were quantified with qPCR following co-administration of OHCs and VD3 analogue (5 μM) (**Tables 1-2**). Analogues that inhibited Hh signaling at 5 μM were evaluated for their ability to regulate Hh and VDR signaling in a concentration-dependent fashion in both the MEFs and the Hh-dependent murine BCC cell line, ASZ001.

Table 1. *In Vitro* Activity of Vitamin D3 Amine Linked Analogues.

	C3H10T1/2			ASZ001	
	% Hh Activity[a,b]	Cyp24A1[a,c]	IC_{50} (μM)[d]	IC_{50} (μM)[d]	Cyp24A1[a,c]
DMSO	1.0	1.0	--	--	1.0
OHCs	100	--	--	--	--
1[g]	35.7 ± 0.3	8,300 ± 40	4.1 ± 0.3	1.1 ± 0.1	2,200 ± 200[e]
2	9.2 ± 0.4[e]	>30,000[e]	0.4 ± 0.1	0.5 ± 0.1	11,000 ± 400[f]
3[f]	30 ± 1	>30,000	3.0 ± 1.0[h]	89.1 ± 41.5[h]	>30,000
5[g]	1.9 ± 0.5	22 ± 5	0.7 ± 0.1	5.2 ± 0.2	1.9 ± 0.1
6[g]	2.5 ± 0.1	7.0 ± 0.9	0.9 ± 0.1	1.8 ± 0.3	1.8 ± 0.2
7[g]	11.6 ± 0.1	17 ± 4	1.0 ± 0.1	1.7 ± 0.1	1.8 ± 0.1
8[g]	0.7 ± 0.2	45 ± 20	0.4 ± 0.1	0.7 ± 0.1	2.7 ± 0.7
9[g]	31 ± 3	3.0 ± 0.5	3.9 ± 0.8	6.3 ± 1.0	1.6 ± 0.2
10[g]	1.3 ± 0.6	21 ± 3	0.3 ± 0.1	0.6 ± 0.2	3.0 ± 0.8
12	98 ± 10	1.2 ± 0.1	---	---	---
13	110 ± 10	1.9 ± 0.5	---	---	---
14	73 ± 7	2.4 ± 0.9	---	---	---
15	110 ± 1	6.1 ± 3.4	---	---	---

16	4.6 ± 0.1	24 ± 1	3.1 ± 0.1	0.3 ± 0.1	1.1 ± 0.7
18	13 ± 8	13 ± 5	3.8 ± 0.7	1.2 ± 0.1	7.8 ± 3.3 [e]
19	1.9 ± 1.6	8.9 ± 1.8	0.6 ± 0.1	0.6 ± 0.1	5.8 ± 0.9 [e]

[a]All analogues evaluated at 5 μM unless otherwise indicated. [b]Values represent % Gli1 mRNA expression relative to OHC control (set to 100%; 20(*S*)-OHC and 22(*S*)-OHC at 5 μM each) after 24 h. [c]Values represent Cyp24A1 mRNA expression compared to DMSO control (set to 1.0). [d]Values represent mean ± SEM for at least two separate experiments performed in triplicate. [e]Compound evaluated at 2.5 μM. [f]Compound evaluated at 1 μM. [g]Previously published results [Ref 13]. [h]Value expressed in nanomolar (nM).

Similar to the SAR results with our previous ester-linked analogues [11], removal or masking of the aromatic hydroxyl group (**12** – **15**) resulted in complete loss of anti-Hh activity (Table 1). More intriguing results were observed when the linker region was extended two atoms. Compared to **8**, amine **16** demonstrated a moderate loss in anti-Hh activity and a slight increase in selectivity. When the arrangement of the linker atoms was reversed (**18** and **19**), the location of the hydroxyl group became more of a contributing factor as **19** (4-phenol) showed greater potency compared to **18** (3-phenol), a trend similar to the ester series. A second noticeable result was the comparable activities for **8** and **19**. Comparing the activities of **8**, **16**, and **19** would suggest that the aromatic A-ring aligns the amine in the linker for key intermolecular binding interactions with the VD3 binding pocket.

Differing results were obtained by incorporating either a hydroxyl or methyl ether on the side chain at C-25 (Table 2). Compared to the non-hydroxylated analogues **7** and **8**, hydroxylation at C-25 (**21** and **22**, respectively), demonstrated comparable anti-Hh activity in the MEFs, but were significantly more active in the ASZ001 BCC cells (IC_{50} value range = 0.11 - 0.22 μM). Hydroxylation at C-25 for these analogues also resulted in enhanced upregulation of Cyp24A1 (15,000 – 30,000 compared to 20- to 40-fold over DMSO), suggesting the hydroxyl moiety significantly improves binding to and activation of VDR. Masking the C-25 hydroxyl as the methyl ether (**25**) reduced both Hh inhibition and VDR activation compared to **21** in both cell lines.

Surprisingly, the addition of the C-25 hydroxyl group (**27**) to the extended linker analogue (**18**) had little effect on Hh inhibition (IC_{50} values ~1 μM) and minimal Cyp24A1 upregulation (10 – 30-fold) in either cell line. Similarly, minimal differences in potency or selectivity were found following C-25 hydroxylation of **19** (analogue **28**) except for a slight increase in Cyp24A1 upregulation in ASZ cells (6-fold vs. 140-fold). Even though no major differences were observed following C-25 hydroxylation, etherification at the C-25 position of **27** (analogue **31**) yielded interesting results. Analogue **31** demonstrated increases in anti-Hh potency as well an increase in upregulation of Cyp24A1 in ASZ cells.

Table 2. Evaluation of C-25 functionalized analogues.

	C3H10T1/2[a]			ASZ001		
	% Hh Activity[a,b]	Cyp24A1[a,c]	IC_{50} (μM)[d]	IC_{50} (μM)[d]	Cyp24A1[c,f]	EC_{50} (μM)[e]
GDC	0.9 ± 0.1	1.6 ± 0.1	82 ± 7 [h]	40 ± 10[h]	0.9 ± 0.2	--
1	35.7 ± 0.3	8,300 ± 40	4.1 ± 0.3	1.1 ± 0.1	2,200 ± 200	0.9 ± 0.1
2	9.2 ± 0.4[f]	>30,000[f]	0.4 ± 0.1	0.5 ± 0.1	11,000 ± 400[g]	0.6 ± 0.1
3[g]	30 ± 1	>30,000	3.0 ± 1.0[h]	89.1 ± 41.5 [h]	>30,000	0.1 ± 0.1
21	5.9 ± 0.9	>30,000	1.3 ± 0.2	0.1 ± 0.1	>30,000	0.1 ± 0.1
22	11 ± 1	15,000 ± 2,000	0.9 ± 0.1	0.2 ± 0.1	>30,000	0.6 ± 0.1
25	3.3 ± 0.7	89 ± 7	2.3 ± 0.1	0.6 ± 0.1	11,000 ± 2,000	0.7 ± 0.1
27	4.1 ± 0.7	34 ± 1	1.7 ± 0.1	1.3 ± 0.1	8.4 ± 2.0	> 10
28	5.6 ± 2.2	6.1 ± 0.4	0.4 ± 0.1	0.5 ± 0.1	140 ± 8	1.3 ± 0.7
31	3.7 ± 0.7	27 ± 4	1.1 ± 0.1	0.7 ± 0.1	2,400 ± 800	0.6 ± 0.1
33	2.9 ± 0.5	27,000 ± 800	1.6 ± 0.1	0.4 ± 0.1	>30,000	0.4 ± 0.6
34	0.7 ± 0.1	14 ± 2	1.6 ± 0.1	1.0 ± 0.2	14 ± 3	>10

[a]All analogues evaluated at 5 μM unless otherwise indicated. [b]Values represent %Gli1 mRNA expression relative to OHC control (set to 100) after 24 h. [c]Values represent Cyp24A1 mRNA expression compared to DMSO control (set to 1.0). [d]Gli1 IC_{50} values represent mean ± SEM for at least two separate experiments performed in triplicate.

[e]Cyp24A1 EC_{50} values represent mean ± SEM for at least two separate experiments performed in triplicate. [f]Compound evaluated at 2.5 μM. [g]Compound evaluated at 1 μM. [h]Value expressed in nanomolar (nM). GDC = Vismodegib or GDC-0449

With significant upregulation of Cyp24A1 observed in both cell lines at a single concentration for several of the 25-OH and 25-OMe analogues, EC_{50} values were obtained in the ASZ001 cells to further determine selectivity for Hh over VDR signaling (Table 2). Interestingly, a strong correlation was observed between Gli1 IC_{50} and Cyp24A1 EC_{50} values for multiple analogues (**21**, **25**, **31**, and **33**). In addition, even analogues that did not correlate as closely in regards to the absolute Gli1 IC_{50} and Cyp24A1 EC_{50} values (**27** - **28**, **34**) followed the overall trend that reduced Hh inhibition is closely associated with reduced VDR activation. Taken together, these results suggested to us a potential role for VDR activation in the regulation of Hh signaling for VD-based compounds, results that were explored further as described below.

Finally, several of the analogues that demonstrated potent Hh-inhibition in the immortalized MEF and ASZ cell lines were evaluated for their anti-proliferative activity in a primary Hh-dependent MB derived from a conditional Patched knockout (Math1-Cre:$Ptch^{fl/fl}$, hereafter called Ptch-CKO) mouse (Table 3) [17-19]. Interestingly, the GI_{50} value for each of these compounds was greater than 1 μM, which is significantly higher than the IC_{50} values for Gli1 down-regulation in the C3H10T1/2 and ASZ cells. Of particular note was the reduced activity of calcitriol (**3**, GI_{50} = 1.4 μM) in the Ptch-CKO cells compared to the immortalized cell lines.

Table 3. *In vitro* activity in primary Ptch-CKO MB cells.

Analogue	GI_{50} (μM)[a]
1	5.8 ± 2.8[b]
3	1.4 ± 0.4
5	>10
10	2.1 ± 0.5

19	2.1 ± 0.7
21	5.3 ± 3.5
22	2.2 ± 1.0
27	1.6 ± 0.5
33	>10

[a]All analogues evaluated following 48 hr incubation.
[b]All values represent Mean ± SEM of at least two separate experiments performed in triplicate.

Select analogues were also evaluated in a series of *in vitro* studies to determine preliminary pharmacokinetic (PK) parameters for this scaffold (Table 4). The first take-away from this study was the overall poor solubility of the compounds, which were essentially insoluble at pH 4.0 and 7.4. This is not a surprising result given the overall hydrophobic nature of the VD3 scaffold. The most soluble compound at pH 4.0 was analogue **22** with a single-atom amine *seco*-B and C-25 hydroxylation, but it demonstrated a significant decrease in solubility at pH 7.4. Analogue **6** with the amide s*eco*-B region was the second most soluble compound at pH 4.0 and maintained solubility at pH 7.4.

Table 4. Pharmacokinetic studies of select analogues.

Cmpd	$T_{1/2}$ (HLM, min)[a]	Clearance (mL/min/mg protein)	Solubility (mg/mL)	
			pH 4.0	pH 7.4
3	>120[b]	ND	ND	ND
5	>231	< 3	1.6×10^{-4}	6.7×10^{-4}
6	>231	< 3	2.7×10^{-4}	6.8×10^{-4}
8	57 ± 0.1	12 ± 0.2	6.2×10^{-7}	2.6×10^{-6}
10	>231	< 3	7.5×10^{-7}	2.6×10^{-7}
19	>231	< 3	1.3×10^{-7}	2.7×10^{-6}
22	31 ± 0.5	22 ± 0.4	2.4×10^{-3}	4.2×10^{-6}
25	>231	< 3	1.7×10^{-5}	1.4×10^{-5}
31	43 ± 7	16 ± 3	6.0×10^{-5}	1.2×10^{-4}
33	47 ± 1	15 ± 0.3	4.8×10^{-5}	3.1×10^{-5}

34	49 ± 7	15 ± 0.3	2.7×10^{-6}	2.3×10^{-6}

[a]Metabolic stability in human liver microsomes (HLM), time until 50% of compound disappeared. [b]Metabolic stability in rat liver homogenate, time until 50% of compound disappeared [Ref 20].

Comparing the results of metabolic stability assays for **8**, **10**, **19** and **22** can provide general conclusions in regards to the overall stability of the amine series of analogues since each of these compounds contain the 4-phenolic A-ring moiety. Looking at compounds **8** and **10**, the only structural difference is the orientation of the *seco*-B region at C-8, where **8** maintains the α-orientation. While both compounds maintain similar solubility, the α-orientation is significantly less stable in human liver microsomes (HLMs) and has a higher clearance rate compared to the β-orientation of **10**. Similarly, the extended amine *seco*-B analogue **19** maintains β-orientation at C-8 and shows a very similar stability profile to the single atom *seco*-B analogue **10**, while the α-orientation of **22** significantly reduces metabolic stability. Addition of the C-25 hydroxyl to **8** (analogue **22**) decreased the half-life and increased the clearance rate while increasing the solubility at pH 4.0. Although **25** has the 3-phenol A-ring, masking of the C-25 hydroxyl group as the methyl-ether increased the half-life significantly and reduced clearance to values similar to the non-functionalized C-25 analogues.

2.3.3. Knockout cell line studies

Multiple reports have suggested both direct and indirect Hh inhibitory mechanisms for vitamin D-based compounds [9-10, 15, 21-22]. Based on our repeated findings that inhibition of Hh signaling correlates with upregulation of VDR activity, we hypothesized that vitamin D-based compounds may inhibit Hh signaling through direct binding to an Hh pathway component, but their anti-Hh activity might also be a downstream result of VDR activation. To further investigate potential crosstalk between the two signaling pathways, a series of studies in several

knockout MEFs and the primary Ptch-CKO cells to evaluate **1**, **3**, **8**, and **22** were performed. Compounds **8** and **22** were chosen because they have similar Gli1 IC_{50} values across cell lines despite significantly different abilities to upregulate Cyp24A1 mRNA.

Initially, we studied the ability of these compounds to regulate Hh and VDR signaling at a single concentration in $VDR^{-/-}$ and $SuFu^{-/-}$ cells (Figure 2). If the vitamin-D based analogues down-regulate Gli1 independently of VDR, then they should maintain their potent Hh inhibition in the $VDR^{-/-}$ MEFs. By contrast, if these analogues regulate Hh signaling at the level of Smo, which has been suggested through several indirect studies [9-10, 15], their ability to down-regulate Gli1 expression should be completely abolished in the $SuFu^{-/-}$ MEFs. Interestingly, the ability of the steroidal compounds to inhibit Hh signaling was significantly reduced, but not completely abolished, in the two knockout lines compared to the wild-type C3H10T1/2 MEFs. By contrast, the known Smo antagonist Vismodegib retained full inhibition of Hh signaling in the $VDR^{-/-}$ MEFs, but was completely inactive in the $SuFu^{-/-}$ MEFs. These results strongly suggest that the vitamin-D based analogues are capable of regulating the Hh pathway through both canonical Hh signaling and VDR. Not surprisingly, the ability of these analogues to up-regulate Cyp24A1 was significantly reduced in the $VDR^{-/-}$ MEFs; however, we also noted decreased up-regulation of Cyp24A1 in the $Sufu^{-/-}$ MEFs.

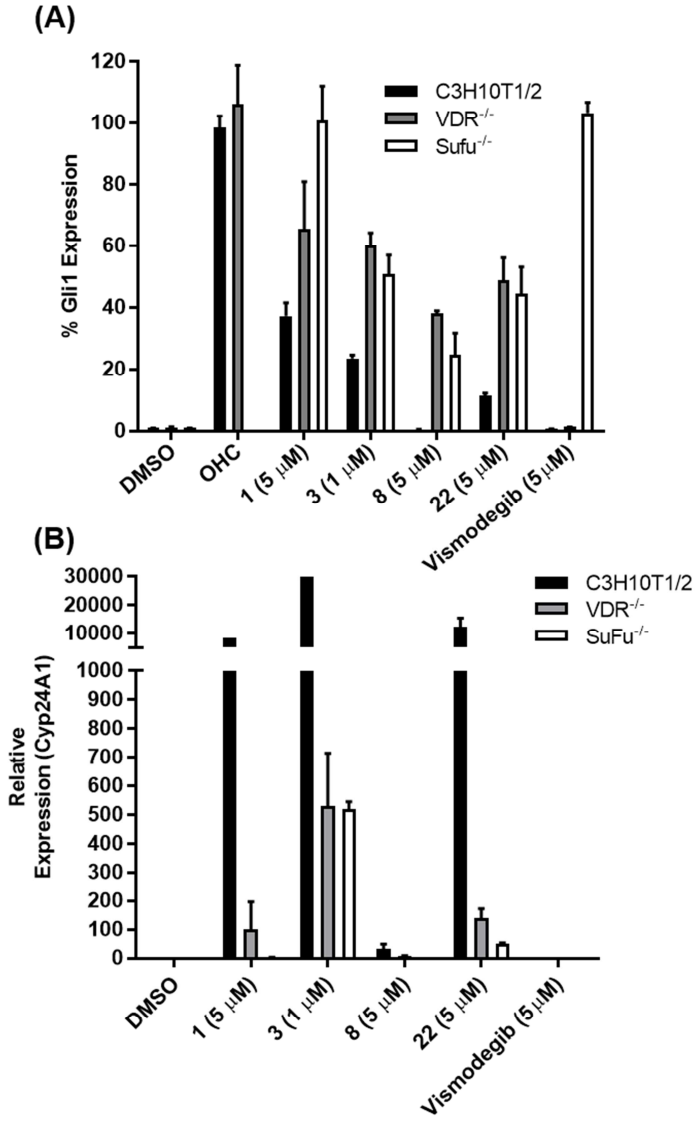

Fig. 2. Effects of VD3-based analogues on VDR and Hh signaling in knockout MEFs. Comparison of Gli1 down-regulation (A) and Cyp24A1 up-regulation (B) across cell lines.

Based on the results of the single concentration studies, we performed full dose-response experiments in both $VDR^{-/-}$ and $Sufu^{-/-}$ MEFs for **1**, **3**, **8** and **22**. Significant decreases in anti-Hh potency and Cyp24A1 up-regulation were observed for **3**, **8** and **22** (Table 5). Calcitriol (**3**) showed the greatest decrease in potency with an IC_{50} of ~3 nM in C3H10T1/2 MEFs and IC_{50} values of ~ 6 – 8 μM in $VDR^{-/-}$ and $Sufu^{-/-}$ cells, respectively. Additionally, Cyp24A1 expression

induced by **3** significantly decreased from the C3H10T1/2 MEFs to the knockout MEFs. Both synthetic analogues demonstrated similar trends in the $VDR^{-/-}$ and $Sufu^{-/-}$ MEFs, i.e. a significant reduction in Hh pathway inhibition in both cell lines compared to the wild-type MEFs. Interestingly, the ability of compound **22** to upregulate Cyp24A1 in the $VDR^{-/-}$ cells provided support for the Sufu/VDR cross-talk mechanism recently proposed [15].

Table 5. ***In vitro*** **activity for select analogues in various MEFs.**

Cmpd	C3H10T1/2		$VDR^{-/-}$		$SuFu^{-/-}$	
	Cyp24A1[a,b]	IC_{50} (μM)[c]	Cyp24A1[a,b]	IC_{50} (μM)[c]	Cyp24A1[a,b]	IC_{50} (μM)[c]
1	8,300 ± 40	4.1 ± 0.3	5.5 ± 0.1	4.5 ± 1.0	2.9 ± 1.0	> 10
3	>30,000[d]	0.0031 ± 0.001	530 ± 200[d]	6.3 ± 1.0	590 ± 70[d]	8.5 ± 3
8	45 ± 20	0.40 ± 0.02	8.1 ± 2	3.9 ± 0.2	1.2 ± 0.1	3.1 ± 0.4
22	15,000 ± 2,000	0.89 ± 0.03	140 ± 30	4.9 ± 0.01	51 ± 5	2.9 ± 0.3

[a]All analogues evaluated at 5 μM unless otherwise indicated. [b]Values represent Cyp24A1 mRNA expression compared to DMSO control (set to 1.0). [c]Gli1 IC_{50} values represent mean ± SEM for at least two separate experiments performed in triplicate. [d]Evaluated at 1 μM.

To determine if the potential for crosstalk between VDR and Hh signaling was specific to the steroidal scaffold or a broader effect of VDR activation, we evaluated the ability of a non-*seco*-steroidal VDR agonist, LG190178 (**35**, Fig. 3), to modulate Hh and VDR signaling in several cell lines (Table 6). In the initial disclosure of **35**, the compound was determined to have lower calcemic effects than **3** while being equipotent as a VDR agonist [23]. Similar to **3**, the non-steroidal agonist **35** significantly up-regulated Cyp24A1 expression in the C3H10T1/2 and ASZ cell lines (Table 5). Unexpectedly, compound **35** was significantly more potent as an Hh pathway inhibitor (sub-nanomolar IC_{50} values) than compound **3** in the MEF and ASZ cells. Finally, a significant reduction in Hh inhibition for both compounds was seen in the $VDR^{-/-}$ cells (low micromolar IC_{50} values).

As noted above, **3** was significantly less active in the Ptch-CKO cells compared to either the C3H10T1/2 or ASZ cells. Similar anti-proliferative results were obtained for compound **35** in the

Ptch-CKO cells (GI_{50} > 10 μM). The reduced anti-Hh activity in the primary cell line correlated well with our results in the $VDR^{-/-}$, which led us to evaluate VDR expression levels in the Ptch-CKO cells. Expression of VDR mRNA was significantly lower in the Ptch-CKO cells compared to normal granule neuron precursors and normal adult cerebellum directly isolated from the mouse, as well as the Hh-dependent NIH3T3 MEF cell line (Supplemental Figure 1). Taken together, the data from the knockout cell lines strongly suggest that inhibition of Hh signaling can be partially attributed to a downstream effect of VDR activation and that these results are not specific to the steroidal scaffold.

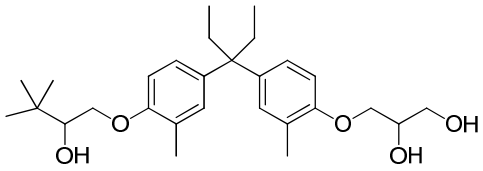

LG190178 (**35**)

Fig. 3. Structure of Non-steroidal VDR agonist LG190178.

Table 6. Comparing the cellular activity of calcitriol (3) and LG190178 (35).

Cmpd	C3H10T1/2[a]		ASZ001[e]			$VDR^{-/-}$ [a]	
	Cyp24A1[a,b]	Gli1 IC_{50} (nM)[c]	Cyp24A1[a,b]	Gli1 IC_{50} (nM)[c]	EC_{50} (nM)[d]	Cyp24A1[a,b]	Gli1 IC_{50} (μM)[c]
3	>30,000	3.1 ± 1.0	>30,000	89.1 ± 41.5	130 ± 1	530 ± 200	6.3 ± 1.0
35	>30,000	0.25 ± 0.04	13,000 ± 2,000	0.23 ± 0.11	7.7 ± 3.2	250 ± 100	1.9 ± 0.2

[a]Compounds evaluated at 1 μM. [b]Values represent Cyp24A1 mRNA expression compared to DMSO control (set to 1.0). [c]IC_{50} (Gli1, nM) and [d]EC_{50} (Cyp24A1, nM) values represent mean ± SEM for at least two separate experiments performed in triplicate.

3. Conclusion

Combining the results contained herein with our previous VD3 SAR studies [11-13], it is clear that the free hydroxyl group of the A-ring is required to maintain anti-Hh activity for the amine-linked analogues; however, the preferred position of the phenol shifted from the 3-

position in the ester/amide series (**5**-**6**, **9**) to the 4-position for the amine-linked analogues (**7**-**8**, **10**). In addition, extension of the single atom amine tether by a single methylene (**16**, **18**-**19**) demonstrated the same preference for the *para*- over the *meta*-phenol. This shift may be due to the slightly increased flexibility of the *seco*-B amine region, which may allow these compounds to better orient the hydroxyl group within the binding site. The more rigid ester and amide *seco*-B analogues are similar to the natural diene system of the vitamin D compounds. As expected, the addition of a hydroxyl moiety at C-25 resulted in significant upregulation of Cyp24A1 mRNA expression across both cell lines for the majority of VD3 analogues, presumably as a result of VDR activation. Taken together with the cellular data, our preliminary PK studies provide additional insight into future analogue development. First, while a specific orientation of the *seco*-B region is not required for Hh inhibition, the β-orientation is more stable. Second, masking the C-25 hydroxyl group may provide a method to balance cellular potency/selectivity and increased microsomal stability.

In addition to the SAR we determined for these vitamin D-based compounds, we noticed a significant correlation between Hh inhibition and VDR activation for several analogues, leading us to explore whether the anti-Hh properties of these compounds are dependent on VDR activation. When select analogues (**1**, **3**, **8**, and **22**) were analyzed in $VDR^{-/-}$ and $Sufu^{-/-}$ MEFs, a significant decrease in anti-Hh was observed; however, inhibition of Hh signaling was not completely abolished. The partial loss in both knockout lines suggests that these compounds may downregulate Gli1 through multiple cellular targets. In addition, as a nuclear receptor, activation of VDR may be able to overcome Sufu knockout by disrupting activation/transcription of Hh target genes. A role for VDR in regulating the Hh pathway is further supported by our findings that the non-secosteroidal VDR agonist **35** is a potent inhibitor of the Hh signaling pathway.

Additional studies to further characterize potential cross-talk between these two cellular pathways is currently underway.

4. Experimental Section

4.1. General information

VD3 used for chemical synthesis was purchased from HBC Chem, Inc. Solvents (anhydrous, ACS or HPLC grade) were purchased from Fisher Scientific or Sigma Aldrich. Column chromatography was performed using silica gel purchased from Sorbtech (Sorbent Technologies). NMR data was collected on a Bruker AVANCE 500 MHz spectrometer using deuterated chloroform ($CDCl_3$, Cambridge Isotope Laboratories, INC), and analysis performed using MestReNova 12.0.0. HRMS data was analyzed at the Mass Spectrometry Facility at the University of Connecticut. Infrared (IR) analysis was performed on a Bruker Alpha Platinum ATR instrument using OPUS software (v 7.2).

4.2. Purity analysis

All compounds analyzed in biological assays were greater than 95% pure based on the following HPLC method. Analogues were dissolved in HPLC grade MeOH (1 mg/mL) and injected (20 – 50 μL) into an Agilent Manual FL-Injection Valve (600 bar) on an Agilent 1100/1200 Series HPLC equipped with a Kinetex 5 μm C18 100Å (150 X 4.6 mm) column and Agilent 1100 Series Photodiode Array Detector. The mobile phase consisted of 95% MeOH/5% H_2O for all analogues with a run time of 10 – 20 min and a flow rate of 1.0 mL/min. Purity was assessed at 254 nm.

4.3. Synthesis of amine seco-B analogues

4.3.1. General reductive amination procedure [13]. Ketone **11** (0.6 mmol) and the requisite amine (1.2 mmol) were dissolved in 1,2-dichloroethane (8 mL). Sodium triacetoxyborohydride (1.8 mmol) was added followed by acetic acid (50 μL) and titanium (IV) isopropoxide (1.2 mmol). The mixture was stirred at RT or reflux for 24 - 48 h. The reaction was quenched with saturated sodium bicarbonate (20 mL) and diluted with diethyl ether (60 mL). The aqueous layer was washed with diethyl ether (3 × 60 mL) and the organic layers combined, dried over anhydrous $MgSO_4$, filtered, and concentrated. Crude residue was purified by column chromatography (SiO_2, 100% Hex to 25% EtOAc in Hex) affording recovery of the starting ketone **11** (20-60%), and the desired amine analogue (15 - 80%).

*4.3.2. (1R,3aR,4S,7aR)-7a-methyl-1-((R)-6-methylheptan-2-yl)-N-phenyloctahydro-1H-inden-4-amine (**12**).* Reductive amination of **11** with aniline provided amine **12**; 65%, 69 mg. HPLC: 95%, R_t = 7.408 min. ^{1}H NMR (500 MHz, $CDCl_3$) δ 7.19 (t, *J* = 7.9 Hz, 2H), 6.68 (t, *J* = 7.3 Hz, 1H), 6.62 (d, *J* = 7.7 Hz, 2H), 3.77 (s, 1H), 2.04 (m, 2H), 1.9-1.5 (9H), 1.41 (m, 3H), 1.31 (m, 3H), 1.17 (m, 5H), 1.07 (m, 1H), 1.00 (m, 3H), 0.97 (d, *J* = 6.7 Hz, 3H), 0.92 (m, 6H). ^{13}C NMR (126 MHz, $CDCl_3$) δ 148.5, 129.2, 129.2, 116.4, 112.5, 56.9, 51.7, 51.1, 45.7, 42.2, 40.3, 39.5, 35.9, 35.4, 30.6, 28.0, 27.1, 23.8, 23.2, 22.8, 22.5, 18.5, 17.9, 13.6. IR (neat) *ν*max 2926, 1600, 1502, 1466, 1428, 1313, 1249, 863. DART-HRMS: *m*/*z* calcd. for $C_{24}H_{39}NO$: 342.3161 $[MH]^+$. Found 342.3132.

*4.3.3. (1R,3aR,4S,7aR)-N-(3-methoxyphenyl)-7a-methyl-1-((R)-6-methylheptan-2-yl)octahydro-1H-inden-4-amine (**13**).* Reductive amination of **11** with *m*-anisidine provided amine **13**; 45%, 23

mg. HPLC: 99%, R_t = 4.062 min. ^{1}H NMR (500 MHz, $CDCl_3$) δ 7.09 (m, 1H), 6.24 (m, 2H), 6.16 (m, 1H), 3.81 (s, 3H), 3.75 (s, 1H), 2.03 (m, 2H), 1.9-1.5 (8H),1.40 (m, 3H), 1.31 (m, 2H), 1.17 (m, 4H), 1.06 (m, 1H), 0.99 (m, 3H),0.96 (m, 3H), 0.92 (m, 6H). ^{13}C NMR (126 MHz, $CDCl_3$) δ 160.9, 149.9, 129.9, 129.8, 105.9, 101.5, 98.4, 56.9, 55.1, 51.7, 51.1, 45.6, 42.2, 40.2, 39.5, 39.4, 36.4, 35.9, 35.4, 35.2, 30.6, 28.04, 28.01, 27.7, 27.1, 24.5, 24.4, 23.8, 23.2, 22.8, 22.5, 20.2. IR(neat) *v*max 2927, 1611, 1493, 1463, 1208, 1159, 1208, 1159, 1050, 829, 750, 686. DART-HRMS: *m*/*z* calcd. for $C_{25}H_{41}NO$: 372.3266; $[MH]^+$. Found 372.3233.

*4.3.4. (1R,3aR,4S,7aR)-N-(4-methoxyphenyl)-7a-methyl-1-((R)-6-methylheptan-2-yl)octahydro-1H-inden-4-amine (**14**).* Reductive amination of **11** with *p*-anisidine provided amine **14**; 42%, 32 mg. HPLC: 99%, R_t = 4.891 min. ^{1}H NMR (500 MHz, $CDCl_3$) δ 6.81 (d, *J* = 8.9 Hz, 2H), 6.59 (d, *J* = 8.8 Hz, 2H), 3.79 (s, 3H), 3.68 (s, 1H), 2.04 (m, 2H), 1.92 (m, 1H), 1.9-1.5 (7H), 1.39 (m, 3H), 1.31 (m, 2H), 1.17 (m, 5H), 1.06 (m, 1H), 1.00 (s, 3H), 0.96 (m, 3H), 0.92 (m, 6H). ^{13}C NMR (126 MHz, $CDCl_3$) δ 151.5, 143.0, 115.0, 113.8, 56.9, 55.9, 52.2, 51.9, 42.2, 40.3, 39.5, 35.9, 35.4, 30.1, 28.0, 27.1, 23.8, 23.2, 22.8, 22.6, 18.5, 17.9, 13.7. IR(neat) *v*max 2928, 2864, 1508, 1464, 1262, 1172, 1041, 814. DART-HRMS: *m*/*z* calcd. for $C_{25}H_{41}NO$: 372.3266; $[MH]^+$. Found 372.3249.

*4.3.5. N-((1R,3aR,4S,7aR)-7a-methyl-1-((R)-6-methylheptan-2-yl)octahydro-1H-inden-4-yl)benzo[d][1,3]dioxol-5-amine (**15**).* Reductive amination of **11** with (3,4-methylenedioxy)-aniline provided amine **15**; 20%, 24 mg. HPLC: 95%, R_t = 5.672 min. ^{1}H NMR (500 MHz, $CDCl_3$) δ 6.68 (d, *J*= 8.3 Hz, 1H), 6.26 (s, 1H), 6.05 (m, 1H), 5.87 (m, 2H), 3.65 (s, 1H), 2.03 (m, 2H), 1.90 (m, 1H), 1.8-1.5 (8H), 1.38 (m, 4H), 1.29 (m, 2H), 1.19 (m, 5H), 1.06 (m, 1H),

0.98 (s, 3H), 0.95 (d, *J* = 6.5 Hz, 3H), 0.92 (m, 6H). ^{13}C NMR (126 MHz, $CDCl_3$) δ 148.3, 144.5, 108.6, 100.4, 95.6, 56.9, 52.2, 51.8, 42.2, 40.3, 39.5, 35.9, 35.4, 30.6, 28.0, 27.1, 23.8, 23.2, 22.8, 22.5, 18.5, 17.8, 13.6. IR(neat) *v*max 3378, 2920, 2860, 1714, 1635, 1600, 1504, 1465, 1377, 1094, 875. DART-HRMS: *m*/*z* calcd. for $C_{25}H_{39}NO_2$: 386.3059 $[MH]^+$. Found 386.3048.

*4.3.6. 4-((((1R,3aR,4S,7aR)-7a-methyl-1-((R)-6-methylheptan-2-yl)octahydro-1H-inden-4-yl)amino)methyl)phenol (**16**).* Reductive amination of **11** with 4-hydroxybenzylamine provided amine **16**; 32%, 10 mg. HPLC: 97%, R_t = 3.399 min. ^{1}H NMR (500 MHz, $CDCl_3$) δ 7.05 (d, *J* = Hz, 2H), 6.78 (d, *J* = Hz, 2H), 5.17 (s, 1H), 3.40 (s, 1H), 3.02 (m, 1H), 2.54 (m, 2H), 2.37 (m, 1H), 2.1-1.9 (3H), 1.75 (m, 2H), 1.67 (m, 5H), 1.55 (m, 2H), 1.48 (m, 2H), 1.35 (m, 3H), 1.15 (m, 3H), 1.06 (s, 3H), 0.90 (m, 9H). ^{13}C NMR (126 MHz, $CDCl_3$) δ 153.9, 131.6, 130.1, 115.2, 59.8, 55.0, 48.8, 39.4, 36.9, 36.7, 35.3, 34.2, 29,7, 28.3, 28.0, 26.2, 24.3, 22.8, 22.5, 22.4, 22.1, 19.1. IR(neat) *v*max 2953, 2922, 2854, 1732, 1685, 1553, 1515, 1455, 1259, 1090, 1011, 799. DART-HRMS: *m*/*z* calcd. for $C_{25}H_{42}NO$: 372.3266 $[MH]^+$. Found 372.3248.

*4.3.7. (1R,3aS,4R,7aR)-7a-methyl-1-((R)-6-methylheptan-2-yl)octahydro-1H-indene-4-carbaldehyde (**17**).* A mixture of methoxymethyl triphenylphosphonium chloride (2.1 g, 6 mmol) in THF (30 mL) was cooled to 0° C. With vigorous stirring, sodium *t*-butoxide (640 mg, 5.7 mmol) was added. The heterogeneous mixture immediately changed color to yellow and on to deeper yellow and finally deep red at 0 ºC. After 30 min, a solution of **11** (400 mg, 1.5 mmol) in THF (10 mL) was added to the above mixture. TLC indicated consumption of **11** after 20 min. Water (80 mL) was added and the mixture was washed with ethyl acetate (3 x 80 mL). The organic layers were combined, dried over anhydrous $MgSO_4$, filtered, and concentrated. The

crude material was purified using column chromatography (SiO_2, 100% Hex to 2% EtOAc in Hex) to yield the vinyl ether; 89%, 390 mg as a clear oil. ^{1}H NMR (500 MHz, $CDCl_3$) δ 5.84 (m, 1H), 3.43 (s, 3H), 1.97 (m, 3H), 1.77 (m, 4H), 1.52 (m, 3H), 1.42 (m, 3H), 1.33 (m, 3H), 1.25 (m, 1H), 1.19 (m, 5H), 1.01 (m, 1H), 0.92 (d, *J* = 6.5 Hz, 3H),0.87 (d, *J* = 6.6 Hz, 3H), 0.86 (d, *J* = 6.6 Hz, 3H), 0.68 (s, 3H). ^{13}C NMR (126 MHz, $CDCl_3$) δ138.9, 118.2, 59.3, 56.0, 52.1, 44.4, 40.4, 39.5, 36.2, 28.0, 27.9, 25.1, 23.8, 22.8, 22.5, 22.4, 21.9, 18.8, 11.6. DART-HRMS: m/z calcd. for $C_{20}H_{37}O$: 293.2844; $[MH]^+$ Found: 293.2849.

The vinyl ether was refluxed in methanol (10 mL) and 3N HCl (5 mL) for 12 h. The reaction was neutralized by the addition of 2 M NaOH, and the aqueous fraction washed with ethyl acetate (3 x 50 mL). The organic layers were combined, dried over anhydrous $MgSO_4$, filtered, and concentrated. The crude material was purified using column chromatography (SiO_2, 100% Hex to 2% EtOAc in Hex) to yield **17** (75%, 280 mg) as a clear oil. ^{1}H NMR (500 MHz, $CDCl_3$) δ 9.55 (m, 1H), 2.30 (m, 1H), 1.99 (m, 1H), 1.86 (m, 1H), 1.78 (m, 1H), 1.66 (m, 2H), 1.53 (m, 2H), 1.30 (m, 8H), 1.12 (m, 5H), 1.02 (m, 1H), 0.93 (d, *J* = 46.5 Hz,3H), 0.87(d, *J* = 2.1 Hz, 3H), 0.86 (d, *J* = 2.0 Hz, 3H), 0.71 (s, 3H). ^{13}C NMR (126 MHz, $CDCl_3$) δ 205.1, 55.4, 50.6, 49.4, 42.7, 39.4, 39.4, 36.1, 35.6, 28.0, 27.8, 25.7, 24.2, 23.7, 22.8, 22.5, 20.7, 18.7, 11.6. DART-HRMS: m/z calcd. for $C_{19}H_{35}O$: 279.2688; $[MH]^+$ Found: 279.2684.

*4.3.8. 3-((((1R,3aS,4R,7aR)-7a-methyl-1-((R)-6-methylheptan-2-yl)octahydro-1H-inden-4-yl)methyl)amino)phenol (**18**).* Reductive amination of **17** with 3-aminophenol provided **18**; 46%, 8.3 mg. HPLC: 99%, R_t = 3.119 min. ^{1}H NMR (500 MHz, $CDCl_3$) δ 7.05 (t, *J* = 8.0 Hz, 1H), 6.22 (m, 2H). 6.13 (s, 1H), 4.50 (bs, 1H), 3.17 (m, 1H), 2.79 (m, 1H), 2.03 (m, 1H), 1.92 (m, 2H), 1.72 (m, 2H), 1.60 (m, 3H), 1.42 (m, 3H), 1.32 (m, 1H), 1.19 (m 5H), (m, 2H), 0.99 (d, *J* =

6.5 Hz, 3H), 0.94 (dd, *J* = 6.6, 2.1 Hz, 6H), 0.74 (s, 3H). ^{13}C NMR (126 MHz, $CDCl_3$) δ 156.8, 150.2, 130.1, 105.9, 104.1, 99.6, 56.2, 53.7, 49.0, 43.2, 40.0, 39.6, 39.5, 36.5, 36.4, 36.2, 35.7, 31.2, 28.1, 28.0, 27.9, 24.6, 24.5, 23.8, 22.8, 22.6, 21.9, 18.7, 11.9. IR(neat) *ν*max 2948, 2923, 2864, 1614, 1508, 1467, 1438, 1333, 1186, 1157, 838. DART-HRMS: *m*/*z* calcd. for $C_{25}H_{42}NO$: 372.3266 $[MH]^+$. Found 372.3270.

*4.3.9. 4-((((1R,3aS,4R,7aR)-7a-methyl-1-((R)-6-methylheptan-2-yl)octahydro-1H-inden-4-yl)methyl)amino)phenol (**19**).* Reductive amination of **17** with 4-aminophenol provided **19**; 38%, 6.2 mg. HPLC: 96%, R_t = 3.384 min. ^{1}H NMR (500 MHz, $CDCl_3$) δ 6.72 (m, 2H), 6.59 (m, 2H), 4.33 (m, 2H), 3.20 (m, 1H), 2.71 (m, 1H), 1.90(m, 4H), 1.72 (m, 2H), 1.57 (m, 3H), 1.41 (m, 5H), 1.30 (m, 2H), 1.18 (m 6H), 1.06 (m, 1H), 0.99 (m, 3H), 0.93 (m, 6H), 0.73 (s, 3H). ^{13}C NMR (126 MHz, $CDCl_3$) δ 116.2, 114.1, 56.2, 53.7, 52.1, 50.1, 45.5, 44.0, 43.1, 39.5, 36.4, 34.8, 31.2, 28.0, 27.6, 25.7, 24.4, 23.8, 22.8, 22.5, 21.9, 20.5, 19.5, 18.7, 11.8. IR(neat) *ν*max 2950, 2923, 2865, 1512, 1468, 1232, 1215, 818. DART-HRMS: *m*/*z* calcd. for $C_{25}H_{42}NO$: 372.3266 $[MH]^+$. Found 372.3268.

4.4. Synthesis of C-25 functionalized single atom nitrogen containing seco-B analogues.

*4.4.1. (1R,3aR,7aR)-1-((R)-6-hydroxy-6-methylheptan-2-yl)-7a-methylhexahydro-1H-inden-4(2H)-one (**20**).* $RuCl_3$ (100 mg, 0.48 mmol) and $NaIO_4$ (1.5 g, 7.0 mmol) were suspended in H_2O (20 mL) with pyridine (40 μL, 0.49 mmol). A solution of **11** (600 mg, 2.3 mmol) in MeCN (20 mL) was added to the reaction mixture and stirred at 60 ºC for 48 h. The mixture was diluted with saturated sodium thiosulfate (20 mL) and filtered through celite. The filtrate was washed

with EtOAc (3 x 50 mL), dried with anhydrous sodium sulfate, and concentrated to afford ketone **20**, which was purified with column chromatography (25% EtOAc in Hex), 420 mg, 67%. ^{1}H (500MHz, $CDCl_3$) δ 2.48 (m, 1H), 2.35-2.23 (2H), 2.15 (m, 1H), 2.06 (m, 1H), 1.93 (m, 2H), 1.77 (m, 1H), 1.65-1.55 (2H), 1.51-1.35 (7H), 1.30 (m, 1H), 1.26 (s, 6H), 1.13 (m, 1H), 1.01 (d, *J* = 6.0 Hz, 3H), 0.68 (s, 3H). ^{13}C NMR (126 MHz, $CDCl_3$) δ 212.0, 71.0, 62.0, 56.6, 49.9, 44.3, 41.0, 39.0, 36.2, 35.5, 29.4, 29.2, 27.5, 24.0, 20.7, 19.1, 18.7, 12.5.

*4.4.2. 3-(((1R,3aR,4S,7aR)-1-((R)-6-hydroxy-6-methylheptan-2-yl)-7a-methyloctahydro-1H-inden-4-yl)amino)phenol (**21**).* Reductive amination of 3-aminophenol with ketone **20** provided amine **21**; 34%, 12 mg. HPLC: 95%, R_t = 2.624 min. ^{1}H NMR (500 MHz, $CDCl_3$) δ 7.01 (t, *J* = 8.0 Hz, 1H), 6.19 (m, 2H), 6.12 (m, 1H), 3.04 (m, 1H), 2.20 (m, 1H), 1.98 (m, 2H), 1.77 (m, 2H), 1.50 (m, 10H), 1.31 (m, 1H), 1.28 (s, 6H), 1.13 (m, 2H), 1.01 (d, *J* = 6.5 Hz, 3H), 0.98 (s, 1H), 0.96 (s, 3H). ^{13}C NMR (126 MHz, $CDCl_3$) δ 156.9, 149.8, 130.1, 106.0, 103.5, 99.3, 71.4, 56.5, 53.4, 45.6, 45.3, 44.3, 36.7, 35.2, 35.2, 33.1, 29.4, 29.3, 29.2, 29.1, 27.7, 24.3, 24.2, 21.3, 20.2, 19.4. IR(neat) *ν*max 3492, 3252, 2916, 1510, 1404, 1245, 1210, 1184, 1155, 962, 816. DART-HRMS: *m*/*z* calcd. for $C_{24}H_{39}NO_2$: 374.3059 $[MH]^+$. Found 374.3068.

*4.4.3. 4-(((1R,3aR,4S,7aR)-1-((R)-6-hydroxy-6-methylheptan-2-yl)-7a-methyloctahydro-1H-inden-4-yl)amino)phenol (**22**).* Reductive amination of 4-aminophenol with ketone **20** provided amine **22**; 29%, 19 mg. HPLC: 99%, R_t = 2.340 min. ^{1}H NMR (500 MHz, $CDCl_3$) δ 6.71 (m, 2H), 6.53 (m, 2H), 2.96 (m, 1H), 2.17 (m, 1H), 1.97 (m, 2H), 1.80 (m, 2H), 1.68 (m, 1H), 1.58 (m, 1H), 1.47 (m, 6H), 1.27 (s, 6H), 1.11 (m, 1H), 1.00 (d, *J* = 6.6 Hz, 3H), 0.95 (s, 3H). ^{13}C NMR (126 MHz, $CDCl_3$) δ 147.4, 116.2, 114.8, 109.9, 71.2, 56.4, 54.9, 45.7, 45.3, 44.3, 36.7,

35.3, 35.2, 33.2, 29.7, 29.4, 29.2, 27.7, 24.5, 24.2, 21.4, 20.2, 19.4. IR(neat) *v*max 3520, 3250, 2915, 1514, 1373,1241, 1189, 1162, 1105, 910, 822. DART-HRMS: *m*/*z* calcd. for $C_{24}H_{39}NO_2$: 374.3059 $[MH]^+$. Found 374.3058.

*4.4.4. (1R,3aR,7aR)-1-((R)-6-methoxy-6-methylheptan-2-yl)-7a-methylhexahydro-1H-inden-4(2H)-one (**23**) and (1R,3aR,5R,7aR)-1-((R)-6-methoxy-6-methylheptan-2-yl)-5,7a-dimethylhexahydro-1H-inden-4(2H)-one (**24**).* Ketone **11** (100 mg, 0.38 mmol) was dissolved in 3 mL anhydrous DMF, capped with a rubber septum and cooled to 0º C. MeI (250 μL, 3.9 mmol) was added followed by NaH (70 mg, 1.1 mmol). The reaction was stirred at 0º C for 2 hrs before warming to RT for 16 hrs, at which time the reaction was quenched with H_2O and extracted with EtOAc (3 x 10 mL). The organic layers were concentrated and purified via column chromatography (SiO_2, 4% EtOAc in hexanes). The reaction yielded both starting material **11** (50 mg, 50 %) along with ketones **23** (27 mg, 25%) and **24** (20 mg, 17%).

Ketone 23. ^{1}H NMR (500 MHz, $CDCl_3$) δ 3.21 (s, 3H), 2.49 (m, 1H), 2.30 (m, 2H), 2.14 (m, 1H), 2.03 (m, 1H), 1.95 (m, 2H), 1.73 (m, 2H), 1.6 – 1.2 (12H), 1.18 (s, 6H), 1.12 (m, 1H), 1.00 (d, *J* = 6.2 Hz, 3H), 0.67 (s, 3H). ^{13}C NMR (126 MHz, $CDCl_3$) δ 212.1, 74.6, 62.0, 56.6, 49.9, 49.1, 40.9, 40.2, 39.0, 36.3, 35.5, 27.5, 25.1, 25.0, 24.0, 20.2, 19.1, 18.7, 12.5.

Ketone 24. ^{1}H NMR (500 MHz, $CDCl_3$) δ3.21 (s, 3H), 2.72 (m, 1H), 2.46 (m, 1H), 2.11 (m, 1H), 1.96 (m, 2H), 1.73 (m, 4H), 1.43 (m, 8H), 1.22 (d, *J* = 7.4 Hz, 3H), 1.18 (m, 6H),1.08 (m, 1H), 1.00 (d, *J* = 6.3 Hz, 3H), 0.68 (s, 3H). ^{13}C NMR (126 MHz, $CDCl_3$) δ 216.0, 74.6, 57.3, 56.6, 49.6, 49.1, 43.7, 40.2, 36.2, 35.5, 35.1, 30.3, 29.7, 27.6, 25.0, 20.1, 19.0, 18.7, 18.5, 13.1.

*4.4.5. 3-(((1R,3aR,4S,7aR)-1-((R)-6-methoxy-6-methylheptan-2-yl)-7a-methyloctahydro-1H-inden-4-yl)amino)phenol (**25**).* Reductive amination of 3-aminophenol with ketone **23** provided amine **25**; 15%, 14 mg. HPLC: 95%, R_t = 2.801 min. ^{1}H NMR (500 MHz, $CDCl_3$) δ 7.02 (m, 1H), 6.16 (m, 3H), 3.73 (s, 1H), 3.23 (m, 3H), 2.02 (m, 2H), 1.9-1.3 (20H), 1.25 (m, 3H), 1.19 (s, 6H), 1.09 (m, 5H), 0.97 (m, 6H), 0.89 (m, 2H). ^{13}C NMR (126 MHz, $CDCl_3$) δ 156.8, 150.1, 130.0, 105.3, 103.3, 99.0, 74.7, 56.7, 51.6, 51.1, 49.1, 42.2, 40.3, 40.2, 36.2, 35.3, 30.6, 29.7, 27.1, 25.0, 23.2, 20.2, 18.5, 17.8, 13.6. IR(neat) *ν*max 2993, 2923, 2852, 1725, 1611, 1559, 1509, 1455, 1363, 1261, 1188, 1085, 814. DART-HRMS: *m/z* calcd. for $C_{25}H_{42}NO_2$: 388.3216 $[MH]^+$. Found. 388.3243.

*4.4.6. (1R,3aS,4R,7aR)-1-((R)-6-hydroxy-6-methylheptan-2-yl)-7a-methyloctahydro-1H-indene-4-carbaldehyde (**26**).* Aldehyde **26** was synthesized following the same procedure described above for **17** starting with ketone **20**; 70% over two steps, 390 mg. Although a mixture of α- and β-aldehydes were formed (2:1 mixture based on the aldehyde proton peak), a single isomer was obtained for each reductive amination procedure. ^{1}H NMR (500 MHz, $CDCl_3$) δ 9.60 (m, 0.5H), 9.53 (m, 1H), 3.47 (m, 0.5H), 3.42 (m, 1H), 1.97 (m, 2H), 1.83 (m, 4H), 1.75 (m, 2H), 1.62 (m, 6H), 1.48 (m, 12H), 1.34 (m, 2H), 1.27 (m, 10H), 1.00 (m, 6H), 0.96 (s, 3H). ^{13}C NMR (126 MHz, $CDCl_3$) δ 205.3, 71.0, 55.4, 52.1, 50.7, 49.5, 47.6, 45.7, 44.3, 43.4, 39.4, 36.6, 35.6, 35.0, 29.7, 29.3, 29.2, 27.5, 25.9, 25.7, 24.2, 23.8, 21.2, 20.7, 19.7, 19.2, 18.7, 11.6.

*4.4.7. 3-((((1R,3aS,4R,7aR)-1-((R)-6-hydroxy-6-methylheptan-2-yl)-7a-methyloctahydro-1H-inden-4-yl)methyl)amino)phenol (**27**).* Reductive amination of 3-aminophenol with aldehyde **26** provided amine **27**; 48%, 15 mg. HPLC: 99%, R_t = 2.375 min. ^{1}H NMR (500 MHz, $CDCl_3$) δ

7.04 (t, *J* = 8.0 Hz, 1H), 6.22 (m, 2H), 6.12 (s, 1H), 4.21 (bs, 1H), 3.20 (m, 1H), 2.77 (m, 1H), 2.02 (m, 1H), 1.89 (m, 2H), 1.70 (m, 2H), 1.57 (m, 3H), 1.39 (m, 3H), 1.31 (m, 1H), 1.18 (m, 8H), 0.98 (d, *J* = 6.5 Hz, 3H), 0.91 (m, 6H), 0.74 (s, 3H). ^{13}C NMR (126 MHz, $CDCl_3$) δ 156.7, 150.3, 130.1, 105.9, 103.9, 99.3, 56., 53.7, 48.9, 43.1, 40.0, 39.5, 36.5, 36.2, 35.7, 31.2, 28.0, 27.9, 24.6, 23.8, 22.8, 22.5, 21.9, 18.7, 11.9. IR(neat) *v*max 2629, 1617, 1510, 1466, 1157, 755, 686. DART-HRMS: *m*/*z* calcd. for $C_{25}H_{42}NO_2$: 372.3266 $[M\text{-}O+H]^+$. Found 372.3380.

*4.4.8. 4-((((1R,3aS,4R,7aR)-1-((R)-6-hydroxy-6-methylheptan-2-yl)-7a-methyloctahydro-1H-inden-4-yl)methyl)amino)phenol (**28**).* Reductive amination of 4-aminophenol with aldehyde **26** provided amine **28**; 59%, 16 mg. HPLC: 95%, R_t = 2.425 min. ^{1}H NMR (500 MHz, $CDCl_3$) δ 6.73 (m, 2H), 6.60 (m, 2H), 4.12 (bs, 1H), 3.189 (m, 1H), 2.78 (m, 1H), 1.98 (m, 1H), 1.90 (m, 2H), 1.71 (m, 2H), 1.57 (m, 3H), 1.38 (m, 4H), 1.18 (m, 7H), 1.05 (m, 1H), 0.97 (d, *J* = 6.5 Hz, 3H), 0.91 (m, 6H), 0.73 (s, 3H). ^{13}C NMR (126 MHz, $CDCl_3$) δ 116.2, 114.4, 56.2, 53.7, 43.1, 40.0, 39.5, 36.4, 36.2, 35.7, 31.2, 28.0, 27.9, 24.6, 23.8, 22.8, 22.5, 21.9, 18.7, 11.8. IR(neat) *v*max 2703, 1635, 1508, 1415, 1155, 804. DART-HRMS: *m*/*z* calcd. for $C_{25}H_{42}NO_2$: 388.3215 $[MH]^+$. Found 388.3214.

*4.4.9. (1R,3aR,7aR,E)-1-((R)-6-methoxy-6-methylheptan-2-yl)-4-(methoxymethylene)-7a-methyloctahydro-1H-indene (**29**).* A mixture of methoxymethyl triphenylphosphonium chloride (1.1 g, 3 mmol) in THF (30 mL) was cooled to 0° C. With vigorous stirring, sodium *t*-butoxide (300 mg, 2.8 mmol) was added. After 30 min, a solution of **20** (210 mg, 0.8 mmol) in THF (10 mL) was added to the above mixture. After 1 hr, TLC indicated consumption. Water (30 mL) was added and the mixture was washed with EtOAc (3 x 30 mL). The organic layers were

combined, dried over anhydrous $MgSO_4$, filtered, and concentrated. The crude 25-OH enol ether was re-suspended in DMF (8 mL) and cooled to 0 ºC. MeI (0.5 mL, 8.0 mmol) was added followed by NaH (100 mg, 1.6 mmol). The mixture was stirred for 4 hr while warming to RT. The reaction was quenched by slow addition of water (20 mL) and the aqueous layer washed with EtOAc (3 x 20 mL). The organics were combined, dried and concentrated. Enol ether **29** was purified via column chromatography (SiO_2, 3% EtOAc in hexanes); 145 mg, 62%. ^{1}H NMR (500 MHz, $CDCl_3$) δ 5.58 (s, 1H), 3.59 (s, 3H), 3.22 (s, 3H), 2.78 (m, 1H), 2.02 (m, 1H), 1.89 (m, 3H), 1.43 (m, 13H), 1.30 (m, 9H), 1.18 (s, 6H), 1.10 (m, 2H), 0.98 (m, 3H), 0.93 (m, 2H), 0.61 (s, 3H). ^{13}C NMR (126 MHz, $CDCl_3$) δ 139.0, 118.3, 74.7, 59.4, 55.9, 52.1, 49.1, 44.4, 40.4, 40.3, 36.5, 36.2, 29.7, 27.9, 25.1, 25.0, 22.5, 22.0, 20.3, 18.8, 11.7.

*4.4.10. (1R,3aS,4R,7aR)-1-((R)-6-methoxy-6-methylheptan-2-yl)-7a-methyloctahydro-1H-indene-4-carbaldehyde (**30**).* Enol ether **29** (100 mg, 0.3 mmol) was dissolved in MeOH (10 mL) and HCl (2N, 5 mL). The mixture was stirred at RT for 6 hr until TLC indicated complete consumption of **29**, at which time the reaction was quenched by slow addition of 2M NaOH before washing with EtOAc (3 x 15 mL). The organic layers were combined, dried and concentrated. Aldehyde **30** was purified via column chromatography (SiO_2, 4% EtOAc in Hex) in good yield (75%, 72 mg). ^{1}H NMR (500 MHz, $CDCl_3$) δ 9.60 (s, 1H), 3.42 (m, 2H), 3.22 (s, 3H), 2.35 (m, 1H), 2.1 – 1.8 (4H), 1.71 (m, 3H), 1.61 (m, 3H), 1.43 (m, 8H), 1.18 (s, 6H), 1.09 (m, 6H), 0.99 (m, 4H), 0.93 (m, 4H), 0.89 (m, 4H), 0.76 (s, 3H). ^{13}C NMR (126 MHz, $CDCl_3$) δ 205.1, 108.8, 74.6, 55.4, 50.7, 49.5, 49.1, 40.3, 39.4, 36.5, 35.7, 31.9, 29.7, 29.3, 27.9, 25.7, 25.0, 24.2, 22.7, 20.7, 20.2, 18.7, 14.1, 11.6. DART-HRMS: *m/z* calcd. for $C_{25}H_{36}O_2$: 291.2688 $[MH]^+$. Found 291.2696.

*4.4.11. 3-((((1R,3aS,4R,7aR)-1-((R)-6-methoxy-6-methylheptan-2-yl)-7a-methyloctahydro-1H-inden-4-yl)methyl)amino)phenol (**31**).* Reductive amination of 3-aminophenol with aldehyde **30** provided amine **31**; 32%, 18 mg. HPLC: 95%, R_t = 2.798 min. ^{1}H NMR (500 MHz, $CDCl_3$) δ 7.04 (m, 1H), 6.21 (m, 2H), 6.15 (m, 1H), 3.23 (s, 3H), 3.17 (m, 1H), 2.79 (m, 1H), 2.02 (m, 1H), 1.89 (m, 2H), 1.71 (m, 2H), 1.58 (m, 3H), 1.42 (m, 7H), 1.24 (m, 2H), 1.19 (s, 6H), 1.1 - 1.0 (4h), 0.99 (m, 3H), 0.92 (m, 3H), 0.73 (s, 3H). ^{13}C NMR (126 MHz, $CDCl_3$) δ 156.9, 130.1, 105.9, 104.1, 99.5, 74.8, 56.1, 53.6, 49.0, 43.1, 40.3, 39.9, 36.5, 36.4, 35.7, 31.2, 29.7, 27.9, 25.0, 24.6, 21.9, 20.2, 18.7, 11.9. IR(neat) *v*max 3490, 2947, 2875, 1780, 1620, 1572, 1512, 1495, 1453, 1365, 1205, 1170, 895. DART-HRMS: *m*/*z* calcd. for $C_{26}H_{43}NO_2$: 402.3372 $[MH]^+$. Found 402.3366.

4.5. Synthesis of C-25 functionalized ester analogues.

*4.5.1. (1R,3aR,4S,7aR)-7a-methyl-1-((R)-6-methyl-6-((triethylsilyl)oxy)heptan-2-yl)octahydro-1H-inden-4-ol (**32**).* Ketone **20** (50 mg, 0.18 mmol) was dissolved in DMF (5 mL) and cooled to 0 ºC. Triethylsilyl chloride (48 mg, 0.44 mmol) was added followed by imidazole (37 mg, 0.54 mmol). The reaction mixture was stirred for 16 hrs at RT. The reaction was quenched by slow addition of water (15 mL) before washing with EtOAc (3 x 10 mL). The organic layers were combined, dried and concentrated. The 25-OTES ketone was purified via column chromatography (SiO_2, 5% EtOAc in Hex; 94%, 66 mg). Sodium borohydride (15 mg, 0.38 mmol) was added to a solution of 25-OTES ketone (60 mg, 0.15 mmol) in DCM:MeOH (2:1, 6 mL) at 0 ºC. The mixture was allowed to warm to RT while stirring for 4 hr. The reaction

mixture was quenched by slow addition of water (10 mL) and washed with EtOAc (3 x 15 mL). The organics were combined, dried and concentrated. Alcohol **32** was purified via column chromatography (SiO_2, 5% EtOAc in Hex; 90%, 60 mg). ^{1}H NMR (500 MHz, $CDCl_3$) δ 4.12 (m, 1H), 2.04 (m, 1H), 1.84 (m, 3H), 1.7 – 1.3 (13H), 1.23 (s, 6H), 1.11 (m, 3H), 0.99 (m, 11H), 0.94 (m, 3H), 0.60 (m, 6H). ^{13}C NMR (126 MHz, $CDCl_3$) δ 73.5, 69.5, 56.7, 52.6, 45.5, 41.8, 40.4, 36.3, 35.3, 33.6, 30.0, 29.8, 27.2, 22.5, 20.8, 18.5, 17.4, 13.5, 7.1, 6.8.

*4.5.2. (1R,4S,7aR)-1-((R)-6-hydroxy-6-methylheptan-2-yl)-7a-methyloctahydro-1H-inden-4-yl 3-hydroxybenzoate (**33**).* Alcohol **32** (20 mg, 0.07 mmol) was dissolved in DCM (10 mL). 3-OMOM-benzoic acid (42 mg, 0.23 mmol) was added followed by DMAP (27 mg, 0.21 mmol) and DCC (37 mg, 0.18 mmol). The reaction mixture was stirred at RT for 16 hr. The mixture was purified directly via column chromatography (SiO_2, 5% EtOAc in Hex; 68%, 21 mg). (±) Camphor sulfonic acid (CSA, 30 mg, 0.13 mmol) was added to a solution of MOM-protected ester (20 mg, 0.04 mol) in MeOH (5 mL) and stirred at RT overnight for 16 hr. Ester **33** was purified via column chromatography (SiO_2, 15% EtOAc in Hex; 75%, 13 mg). HPLC: 97%, R_t = 2.229 min. ^{1}H NMR (500 MHz, $CDCl_3$) δ 7.62 (m, 2H), 7.34 (t, *J* = 7.9 Hz,1H), 7.11 (m, 1H), 5.42 (s, 1H), 2.05 (m, 2H), 1.84 (m, 3H), 1.6 – 1.4 (10H), 1.28 (s, 6H), 1.23 (m, 2H), 1.16 (m, 1H), 1.04 (s, 3H), 0.96 (d, *J* = 6.5 Hz, 3H). ^{13}C NMR (126 MHz, $CDCl_3$) δ 166.7, 156.2, 132.1, 129.6, 121.6, 120.2, 116.3, 72.7, 71.6, 56.4, 51.5, 44.2, 41.9, 39.9, 36.1, 35.4, 30.5, 29.3, 29.2, 27.0, 22.6, 20.8, 18.5, 18.0, 13.6. IR(neat) *v*max 2939, 1717, 1687, 1588, 1452, 1291, 1215, 1156, 1102, 1072, 946, 917, 883, 804, 752. DART-HRMS: m/z calcd. for $C_{25}H_{38}O_4$: 420.3114 $[MNH4]^+$. Found 420.3104.

*4.5.3. (1R,3aR,4S,7aR)-1-((R)-6-methoxy-6-methylheptan-2-yl)-7a-methyloctahydro-1H-inden-4-yl 3-hydroxybenzoate (**34**).* Sodium borohydride (13 mg, 0.32 mmol) was added to a solution of ketone **23** (25 mg, 0.08 mmol) in MeOH (5 mL). After 2 hr, the reaction was quenched with water and washed with EtOAc (3 x 15 mL). The organics were combined and concentrated. 25-OMe Grundmann's alcohol (25-OMe GA) was purified via column chromatography (8% EtOAc in Hex; 92%, 23 mg). ^{1}H NMR (500 MHz, $CDCl_3$) δ 4.11 (m, 1H), 3.21 (s, 3H), 2.05 (m, 1H), 1.87 (m, 3H), 1.59 (m, 1H), 1.40 (m, 12H), 1.21 (m, 1H), 1.17 (s, 6H), 1.07 (m, 2H), 0.97 (s, 3H), 0.94 (d, *J* = 6.5 Hz, 3H). ^{13}C NMR (126 MHz, $CDCl_3$) δ 74.7, 69.4, 56.6, 52.6, 49.0, 41.8, 40.4, 40.3, 36.3, 35.2, 33.6, 27.1, 25.04, 25.02, 22.5, 20.2, 18.5, 17.4, 13.5.

25-OMe GA (20 mg, 0.07 mmol) was dissolved in DCM (10 mL). 3-OMOM-benzoic acid (42 mg, 0.23 mmol) was added followed by DMAP (27 mg, 0.21 mmol) and DCC (37 mg, 0.18 mmol). The reaction mixture was stirred at RT overnight for 16 hr. The reaction mixture was purified directly via column chromatography (SiO_2, 5% EtOAc in Hex; 68%, 21 mg). ^{1}H NMR (500 MHz, $CDCl_3$) δ 7.78 (m, 1H), 7.75 (m, 1H), 7.40 (t, *J* = 7.9 Hz, 1H), 7.26 (m, 1H), 5.44 (m, 1H), 5.25 (s, 2H), 3.53 (s, 3H), 3.22 (s, 3H), 2.10 (m 1H), 2.02 (m, 1H), 1.87 (m, 2H), 1.57 (m, 5H), 1.42 (m, 6H), 1.30 (m, 4H), 1.18 (s, 6H), 1.09 (s, 3H), 0.99 (d, *J* = 6.5 Hz, 3H). ^{13}C NMR (126 MHz, $CDCl_3$) δ 166.1, 157.2, 132.3, 129.4, 123.1, 120.8, 117.2, 94.5, 74.6, 72.4, 56.4, 56.0, 51.6, 49.1, 41.9, 40.3, 39.9, 36.3, 35.4, 30.5, 27.1, 25.0, 22.6, 20.2, 18.6, 18.0, 13.5.

(±) Camphor sulfonic acid (CSA, 30 mg, 0.13 mmol) was added to a solution of MOM-protected ester (20 mg, 0.04 mol) in MeOH (5 mL) and stirred at RT overnight for 16 hr. The mixture was concentrated and purified via column chromatography (SiO_2, 8% EtOAc in Hex) to yield **34** (65%, 14 mg). HPLC: 95%, R_t = 2.918 min. ^{1}H NMR (500 MHz, $CDCl_3$) δ 7.66 (m, 1H), 7.61 (s, 1H), 7.35 (t, *J* = 7.9 Hz, 1H), 7.10 (m, 1H), 6.48 (s, 1H), 5.42 (s, 1H), 3.25 (s, 3H),

2.08 (m, 2H), 1.84 (m, 2H), 1.56 (m, 5H), 1.42 (m, 5H), 1.30 (m, 3H), 1.21 (s, 6H), 1.05 (s, 3H), 0.97 (d, J = 6.5 Hz, 3H). ^{13}C NMR (126 MHz, $CDCl_3$) δ 166.6, 156.1, 132.2, 129.6, 121.7, 120.1, 116.2, 75.1, 72.7, 56.4, 51.5, 49.0, 41.9, 40.4, 39.9, 36.2, 35.4, 30.5, 27.0, 25.0, 24.8, 22.7, 20.3, 18.6, 18.0, 13.6. IR(neat) *v*max 2982, 2940, 1715, 1686, 1588, 1450, 1290, 1216, 1157, 1098, 1066, 946, 918, 881, 805, 753. DART-HRMS: m/z calcd. for $C_{26}H_{40}O_4$: 434.3270 $[MNH_4]^+$. Found 434.3276.

4.6. Biological evaluation

4.6.1. General information and cellular studies

Protocols for general cell culture and qPCR (Hh pathway and VDR) are as described previously [11-14]. Protocols for the initiation and propagation of primary Math1-Cre;$Ptc^{fl/fl}$ medulloblastoma tumors, tumor cell isolation and *in vitro* culture of Ptch-CKO MB cells, as wells as the proliferation and qPCR studies performed in these cells were as previously described [17-19]. 20α-Hydroxycholesterol and 22(S)-hydroxycholesterol (OHCs) were purchased from Sigma-Aldrich. GDC (Vismodegib, GDC-0449) was utilized as a clinical standard and purchased from Caymen Chemical. VD3 for biological studies was purchased from Sigma-Aldrich and calcitriol was purchased from Caymen Chemical. Data was analyzed using GraphPad Prism 5, and reported values represent mean ± SEM for at least two separate experiments performed in triplicate.

4.6.2. Preliminary pharmacokinetic assays

The solubility and stability of VD3 and analogues were determined through standard protocols as a contract research service by Pharmaron, Inc. Kineitc solubility of each compound was assessed

in PBS at pH 4.0 and 7.4. Metabolic stability (1 μM, human liver microsomes) was determined at various time points to provide an *in vitro* half-life ($T_{1/2}$) that was converted into the *in vitro* intrinsic clearance (CL_{int}). For each assay, compound concentrations was determined via LC-MS/MS on a Waters XEVO® TQ-D equipped with an Acquity UPLC.

ACKNOWLEDGMENTS

The authors gratefully acknowledge support of this work by the V Foundation for Cancer Research (V Scholar, M.K.H.), the Charles H. Hood Foundation, the University of Connecticut Research Foundation, and the American Cancer Society (RSG-13-131-01). ASZ001 cells were kindly provided by Dr. Ervin Epstein (Children's Hospital Oakland Research Institute). $VDR^{-/-}$ cells were kindly provided by Dr Jun Sun (University of Illinois at Chicago). $Sufu^{-/-}$ cells were kindly provided by Dr. Matthew Scott (Stanford University). LG190178 (**35**) was kindly provided by Dr. Alexander (Leggy) Arnold (University of Wisconsin-Milwaukee).

Appendix A. Supplementary data. NMR Spectra and HPLC chromatograms for key intermediates and all final analogues. These data can be found at

References

[1] E.H. Epstein, Basal cell carcinomas: attack of the hedgehog. Nat. Rev. Cancer 8 (2008) 743-754.

[2] M. K. Hadden, Hedgehog pathway agonism: Therapeutic potential and small-molecule development. ChemMedChem 9 (2014) 27-37.

[3] F. Wu, Y. Zhang, B. Sun, A.P. McMahon, Y. Wang, Hedgehog signaling: From basic biology to cancer therapy. Cell Chem. Biol. 24 (2017) 252-280.

[4] R.L. Yauch, G.J. Dijkgraaf, B. Alicke, T. Januario, C.P. Ahn, T. Holcomb, K. Pujara, J. Stinson, C.A. Callahan, T. Tang, J.F. Bazan, Z. Kan, S. Seshagiiri, C.L. Hann, S.E. Gould, J.A. Low, C.M. Rudin, F.J. de Sauvage, Smoothened mutation confers resistance to a hedgehog pathway inhibitor in medulloblastoma, Science 326 (2009) 572-574.

[5] A.L.S. Chang, A.E. Oro, Initial Assessment of tumor regrowth after vismodegib in advanced basal cell carcinoma, Arch Dermatol. 148 (2012) 1324-1325.

[6] A. Gonnissen, S. Isebaert, K. Haustermans, Targeting the hedgehog signaling pathway in cancer: beyond Smoothened. Oncotarget 6 (2015) 13899-13913.

[7] V. Veldurthy, R. Wei, L. Oz, P. Dhawan, Y.-H. Jeon, S. Christakos, 2016. Vitamin D, calcium homeostasis and aging. Bone Research 4, 16041.

[8] M.J. Larriba, J. M. Gonzalez-Sancho, F. Bonilla, A. Munoz, Interaction of vitamin D with membrane-based signaling. Front. Physiol. 5 (2014) 60.

[9] M.F. Bijlsma, C.A. Spec, D. Zivkovic, S. van de Water, F. Rezaee, M.P. Peppelenbosch, Repression of smoothened by patched-dependent (pro-)vitamin D3 secretion. PLoS Biol. 4 (2006) e232.

[10] J.Y. Tang, T.Z. Xiao, Y. Oda, K.S. Chang, E. Shpall, A. Wu, P.-L. So, J. Hebert, D. Bikle, E.H. Epstein, Vitamin D3 inhibits hedgehog signaling and proliferation in murine basal cell carcinomas, Cancer Prev. Res. 4 (2011) 744-751.

[11] A.M. DeBerardinis, D. Madden, U. Banerjee, V. Sail, D.S. Raccuia, D. De Carlo, S. Lemieux, A. Meares, M.K. Hadden, Structure-activity relationships for vitamin D3-based

aromatic A-ring analogues as hedgehog pathway inhibitors, J. Med. Chem. 57 (2014) 3724-3736.

[12] U. Banerjee, A.M. DeBerardinis, M.K. Hadden, Design, synthesis, and evaluation of hybrid vitamin D3 side chain analogues as hedgehog pathway inhibitors. Bioorg. Med. Chem. 23 (2015) 548-555.

[13] A.M. DeBerardinis, D.S. Raccuia, E.N. Thompson, C.A. Maschinot, M.K. Hadden, Vitamin D3 analogues that contain modified A- and seco-B rings as hedgehog pathway inhibitors. Euro. J. Med. Chem. 93 (2015) 156-171.

[14] C.A. Maschinot, M.K. Hadden, Synthesis and evaluation of vitamin D3 analogues with C-11 modifications as inhibitors of hedgehog signaling. Bioorg. Med. Chem. Lett. 27 (2017) 4011-4014.

[15] F. Alimirah, X. Peng, A. Gupta, L. Yuan, J. Welsh, M. Cleary, R.G. Mehta, Crosstalk between the vitamin D receptor (VDR) and miR-214 in regulating SuFu, a hedgehog pathway inhibitor in breast cancer cells. Exp. Cell Res. 349 (2016) 15-22.

[16] E. McNeill, J. Du Bois, Ruthenium-catalyzed hydroxylation of unactivated tertiary C-H bonds. J. Am. Chem. Soc. 132 (2010) 10202-10204.

[17] Z.-J. Yang, T. Ellis, S.L. Markant, T.-A. Read, J.D. Kessler, M. Bourboulas, U. Schüller, R. Machold, G. Fishell, D.H. Rowitch, B.J. Wainwright, R.J. Wechsler-Reya, Medulloblastoma can be initiated by deletion of patched in lineage-restricted progenitors or stem cells. Cancer Cell 14 (2008) 135−145.

[18] S.L. Markant, L.A. Esparza, J. Sun, K.L. Barton, L.M. McCoig, G.A. Grant, J.R. Crawford, M.L. Levy, P.A. Northcott, D. Shih, M. Remke, M.D. Taylor, R.J. Wechsler-

Reya, Targeting sonic hedgehog-associated medulloblastoma through inhibition of aurora and polo-like kinases. Cancer Res. 73 (2013) 6310−6322.

[19] S.N. Brun, S.L. Markant, L.A. Esparza, G. Garcia, D. Terry, J.-M. Huang, M.S. Pavlyukov, X.-N. Li, G.A. Grant, J.R. Crawford, M.L. Levy, E.M. Conway, L.H. Smith, I. Nakano, A. Berezov, M.I. Greene, Q. Wang, R.J. Wechsler-Reya, Survivin as a therapeutic target in sonic hedgehog-driven medulloblastoma. Oncogene 34 (2015) 3770−3779.

[20] O. Werz, H. Wiesinger, A. Steinmeyer, D. Steinhilber, New vitamin D receptor agonists with decreased metabolic stability. Biochem. Pharma. 59 (2000) 1597-1601.

[21] A. Uhmann, H. Niemann, B. Lammering, C. Henkel, I. Heb, F. Nitzki, A. Fritsch, N. Prüfer, A. Rosenberger, C. Dullin, A. Schraepler, J. Reifenberger, S. Schweyer, T. Pietsch, F. Strutz, W. Schulz-Schaeffer, H. Hahn, Antitumoral effects of calcitriol in basal cell carcinomas involve inhibition of hedgehog signaling and induction of vitamin D receptor signaling and differentiation. Mol. Cancer Ther. 10 (2011) 2179−2188.

[22] A.E. Teichert, H. Elalieh, P.M. Elias, J. Welsh, D.D. Bikle, Overexpression of hedgehog signaling is associated with epidermal tumor formation in vitamin D receptor-null mice. J. Invest. Dermatol. 131 (2011) 2289-2297.

[23] M.F. Boehm, P. Fitzgerald, A. Zou, M.G. Elgort, E.D. Bischoff, L. Mere, D.E. Mais, R.P. Bissonnette, R.A. Heyman, A.M. Nadzan, M. Reichman, E.A. Allegretto, Novel nonsecosteroidal vitamin D mimics exert VDR-modulating activities with less calcium mobilization than 1,25-dihydroxyvitamin D3. Chem. Biol. 6 (1999)265-275.

[24] C. Carlberg, M.J. Campbell, Vitamin D receptor signaling mechanisms: Integrated actions of a well-defined transcription factor. Steroids 78 (2013) 127-136.

Table of Contents Graphic:

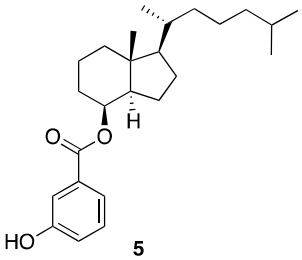

5

Hh - IC_{50} = 5.2 ± 0.2 μM
VDR - EC_{50} = 1.9 ± 0.1 μM

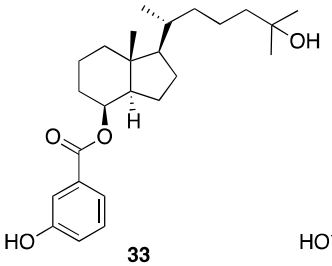

33

Hh - IC_{50} = 0.4 ± 0.1 μM
VDR - EC_{50} = 0.4 ± 0.1 μM

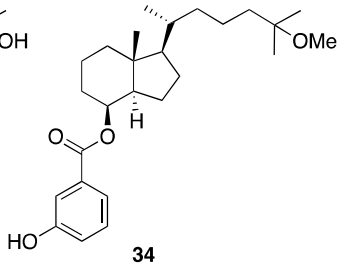

34

Hh - IC_{50} = 1.0 ± 0.2 μM
VDR - EC_{50} = > 10 μM

Highlights

1. A new series of vitamin D3 analogues with modifications to C-25 were designed and synthesized.

2. Analogues containing a C-25 hydroxyl are inhibitors of Hedgehog (Hh) signaling and activators of the vitamin D receptor.

3. Analogues 16, 21, and 22 demonstrated low nanomolar inhibition of pathway signaling in Hh-dependent basal cell carcinoma.

4. Activation of the vitamin D receptor correlates to enhance down-regulation of Gli1 expression.